J Mater Sci: Mater Med (2009) 20:1795–1801
DOI 10.1007/s10856-009-3753-x

Mechanical properties of organically modified silicates for bone regeneration

Miguel Manzano · Antonio J. Salinas · Francisco J. Gil · María Vallet-Regí

Received: 28 November 2008 / Accepted: 15 April 2009 / Published online: 29 April 2009

Abstract In this paper, different organic–inorganic hybrid materials based in the $CaO–SiO_2$–poly(dimethyl siloxane) PDMS system have been characterised by means of nanoindentation and their static mechanical properties (Young's modulus, and hardness) have been investigated. These mechanical properties have been discussed in relation to the chemical composition and structure of the different hybrid materials. Besides, the mechanical behaviour of hybrid materials is visco-elastic and it therefore presents phenomena of creep that will be influenced by the temperature of the mechanical test; undoubtedly, a temperature of 37°C accelerates the processes of creep.

1 Introduction

The bioceramics research area has grown intensively on the last few years due to the increase of incidence of bone diseases in modern societies. Among the materials investigated, some ceramics like bioactive glasses can bond to hard tissues when implanted in human bodies [1, 2]. However, their application in biomedical technologies has been reduced to low stress areas because of their poor mechanical properties typical from glasses and ceramics. On the other hand, polymers like silicone rubber have been used as substitutes for soft tissues, but they become surrounded by a fibrous tissue when embedded in the body, so their usage as biomaterials is also limited. Organically modified silicates (ormosils) are a type of organic–inorganic hybrid materials that can combine the bioactive properties of inorganic glasses and the mechanical properties of organic polymers. It is generally accepted that the bone bonding mechanism depends on the formation of an apatite layer on the surface of a material when in contact with physiological fluids. Also the presence of calcium ions and silanol groups on the material plays an important role in the formation of the apatite layer. Thus, $CaO–SiO_2$–poly(dimethylsiloxane) (PDMS) ormosils would combine the bioactive response of glass-like materials, presence of Ca^{2+} ions and silanol groups, and the mechanical properties of silicone-like polymers [3, 4].

In a previous investigation, the bioactive response of $CaO–SiO_2$–PDMS ormosils was improved with the introduction of P at molecular level by using diethyl phosphatoethyl triethoxysilane (DEPETES) as additive during the synthesis (Fig. 1) [5]. The mechanical properties of these PDMS–$CaO–SiO_2$–phosphatoethylsilane (PES) ormosils will be here investigated. On the other hand, a possible heterogeneous distribution of the material could be observed when large amounts of PDMS were used. To obtain a more homogeneous distribution of the organic content throughout the hybrid network, the precursor monomer of PDMS (dimethyl diethoxysilane [DDS]) was used in a previous work [5] to produce the polymerisation in situ (Fig. 2). Bioactive ormosils were then obtained and their mechanical properties will be here described.

M. Manzano · A. J. Salinas (✉) · M. Vallet-Regí (✉)
Departamento de Química Inorgánica y Bioinorgánica,
Facultad de Farmacia, Universidad Complutense de Madrid,
28040 Madrid, Spain
e-mail: salinas@farm.ucm.es

M. Vallet-Regí
e-mail: vallet@farm.ucm.es
URL: www.ucm.es/info/inorg/

M. Manzano · A. J. Salinas · M. Vallet-Regí
Centro de Investigación Biomédica en Red: Bioingeniería,
Biomateriales y Nanomedicina, CIBER-BBN, Madrid, Spain

F. J. Gil
Departamento Ciencia de Materiales e Ingeniería Metalúrgica,
ETSEIB, Universidad Politécnica de Cataluña, Barcelona, Spain

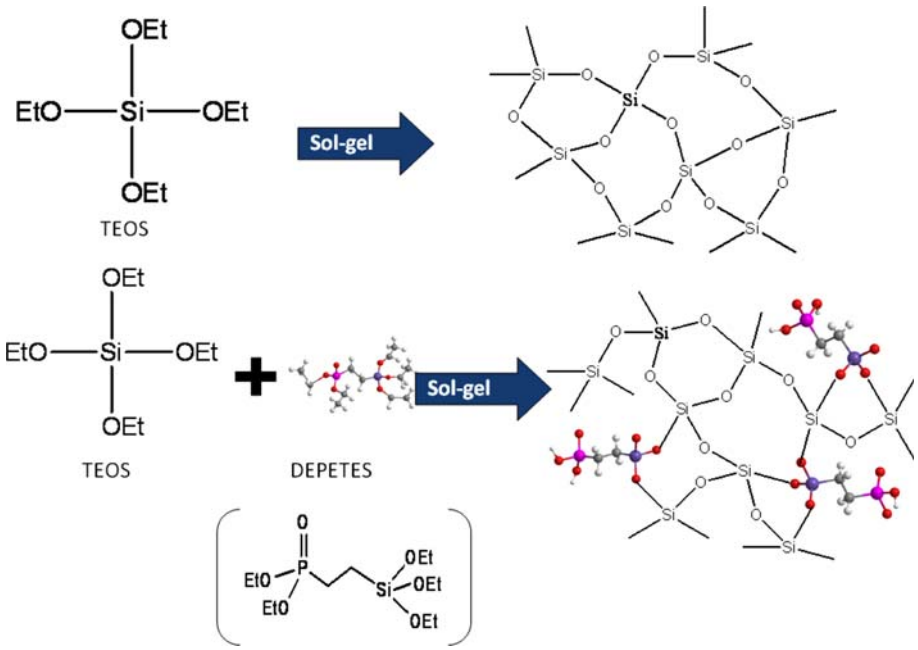

Fig. 1 Sol–gel formation of a pure SiO_2 network (*top*) and a network including phosphorus chemically bonded to silicon via a $–CH_2–CH_2–$ bridge (*bottom*). Additions of Ca^{2+} in the synthesis ensured a bioactive behavior of the ormosils that was improved by the presence of P

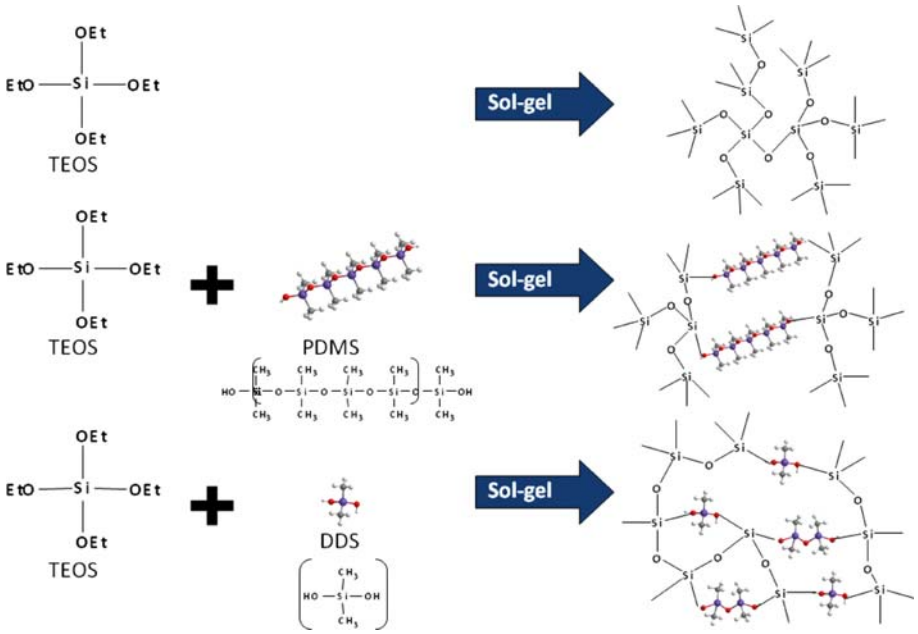

Fig. 2 Formation of a silica network (*top*) and organic–inorganic networks condensing TEOS with oligomeric PDMS (*center*) or monomeric DDS (*bottom*). In this case more homogeneous materials were obtained. Inclusions of Ca^{2+} promoted the bioactive response of ormosils

However, to use these hybrids as biomaterials, their mechanical properties (hardness, elastic modulus and creep) are very important for biomechanical considerations and long-term behaviour [6]. Nanoindentation has been the technique used in this study. The creep produced over time was obtained by application of different levels of constant stress. The samples were stressed at different values which are the values at which the biomaterial could be stressed in clinical use for the repair of hard tissues. Laws have been here obtained to model the visco-elastic behaviour at different stress for these materials.

2 Materials and methods

2.1 Reagents

Tetraethyl orthosilicate (TEOS) (Aldrich), poly(dimethylsiloxane) hydroxyl-terminated (PDMS, $M_n = 550$ g mol^{-1}) (Sigma–Aldrich), dimethyl diethoxysilane (DDS) (Fluka), diethyl phosphatoethyl triethoxysilane (DEPETES) (Gellest Inc.), calcium nitrate tetrahydrate (Sigma–Aldrich), 2-Propanol (Sigma–Aldrich), reagent grade hydrochloric acid (Panreac) and reagent grade nitric acid (Sigma–Aldrich) were all used as received.

2.2 Synthesis of PDMS–CaO–SiO_2–PES ormosils

Figure 3 shows the synthesis path for the preparation of PDMS–CaO–SiO_2–PES ormosils which will be named as NP_{x-y} hybrids, where N stands for the calcium source (calcium nitrate tetrahydrate), P stands for the presence of phosphorous within the structure, x represents the amount of DEPETES and y is the proportion of water. Measured amounts of TEOS, PDMS, DEPETES and 2-Propanol (Table 1) were magnetically stirred at room temperature. The compositions here selected are known to be bioactive when soaked in SBF for 7 days [5]. Separately, calcium nitrate tetrahydrate was dissolved at room temperature into a 2 M nitric acid aqueous solution in the amounts shown in Table 1. Then both solutions were mixed together and magnetically stirred for 1 h at room temperature. After this, the solution was introduced into a sealed poly(tetrafluoroethylene) (PTFE) container and gelled for 24 h at room temperature, aged for 7 days at 60°C and dried for 7 days at 100°C.

2.3 Synthesis of CaO–SiO_2–PDMS ormosils

Figure 4 shows the synthesis path for the preparation of CaO–SiO_2–PDMS ormosils, which would be named as H_{N-x}, where H stands for hybrid, N for the calcium source

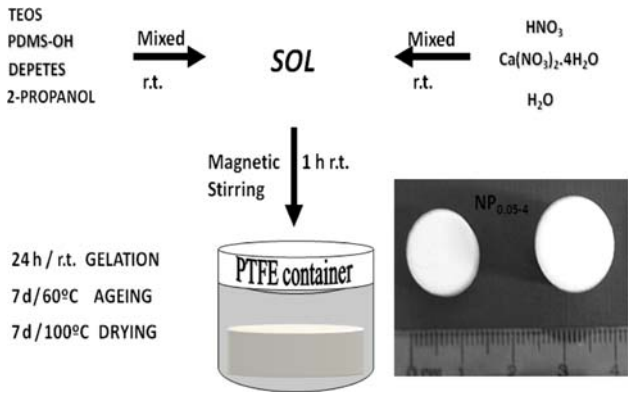

Fig. 3 Procedure followed for synthesizing PDMS–CaO–SiO_2–PES ormosils. A take pictures of monoliths of this series is also included

Table 1 Molar ratio of the precursors employed for the synthesis of PDMS–CaO–SiO_2–PES ormosils

Material	TEOS	DEPETES	H_2O	$Ca(NO_3)_2 \cdot 4H_2O$	PDMS
$NP_{0.05-4}$	1	0.05	4	0.10	0.33
$NP_{0.10-2}$	1	0.10	2	0.10	0.33
$NP_{0.10-3}$	1	0.10	3	0.10	0.33
$NP_{0.10-4}$	1	0.10	4	0.10	0.33

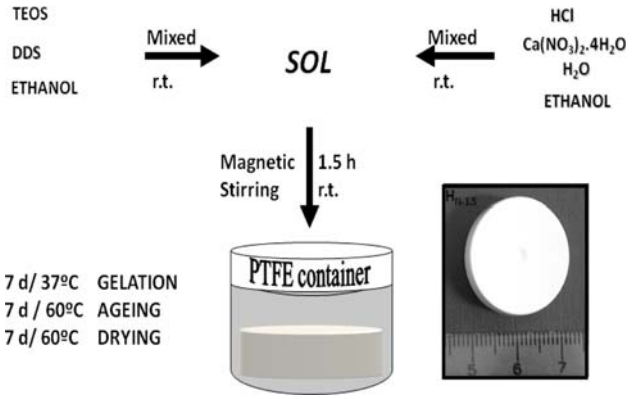

Fig. 4 Procedure followed for synthesizing CaO–SiO_2–PDMS ormosils using DDS as precursor of PDMS. A photograph of a monolith of this series is also included

(calcium nitrate) and x represents the amount of DDS present. Different molar ratios of TEOS and DDS were mixed in ethanol as shown in Table 2. These compositions were selected because they are known to be bioactive [5]. In a different vessel calcium nitrate tetrahydrate was dissolved in a hydrochloric acid solution (1 M) and 5 ml of ethanol. When everything was homogeneously dissolved, both solutions were mixed and the resultant sol was magnetically stirred for 1.5 h at room temperature. After this, the solution was poured into a PTFE sealed vessel and gelled at 37°C for 7 days, aged at 60°C for 7 days and dried at 60°C for further 7 days.

2.4 Materials characterisation

Fourier transformed infrared (FTIR) spectroscopy was recorded using a ThermoNicolet Nexus equipped with a Goldengate Attenuated Total Reflectance (ATR). A JEOL 6400 microscope coupled with a LINK 10000 device was used to carry on the Scanning Electron Microscopy (SEM) and Energy Disperse X-ray Spectroscopy (EDS).

2.5 In vitro studies

To investigate the bioactive behaviour of the materials, the produced monoliths were soaked into a Simulated Body Fluid (SBF), which is a solution proposed by Kokubo et al. [7] and consists of an acellular solution with ionic composition similar to human plasma. The molar ratio surface area/volume of SBF was kept constant. Thus, for pieces with around 4 cm^2 of external surface, 40 ml of SBF were used in each experiment. After 7 days in SBF at 37°C, the samples were rinsed with acetone and water, dried and analysed by FTIR, SEM and EDS. When a new layer, mainly composed of Ca and P, was formed, the specimen was considered bioactive.

Table 2 Molar ratio of the precursors employed for the synthesis of $CaO–SiO_2$–PDMS ormosils

Material	TEOS	DDS	H_2O	$Ca(NO_3)_2 \cdot 4H_2O$
$H_{N-0.25}$	1	0.25	5	0.10
H_{N-1}	1	1	5	0.10
$H_{N-1.5}$	1	1.5	5	0.10

2.6 Mechanical properties

In an indentation test, the hardness is defined as the indentation load divided by the projected contact area, as shown in Eq. 1. The elastic modulus of the sample can be calculated based on the relationship developed by Sneddon [8] as illustrated in Eq. 2:

$$H = \frac{P_{\max}}{A} \tag{1}$$

$$S = 2\beta\sqrt{\frac{A}{\pi}}E_r \tag{2}$$

where A is the projected contact area between the indenter and the sample surface at the maximum load, $P_{\max}$; S is the contact stiffness of material; β is a constant depending on the geometry of the indenter; and E_r is the reduced elastic modulus which is calculated from Eq. 3:

$$\frac{1}{E_r} = \frac{1-v^2}{E} + \frac{1-v_i^2}{E_i}. \tag{3}$$

In above equation, E_i (1140 GPa) and v_i (0.07) are the elastic properties of the diamond indenter. E and v are the elastic modulus and Poisson's ratio of the sample. A three-side pyramid (Berkovich) diamond indenter was employed for the indentation experiments. For a perfectly sharp Berkovich indenter, the projected area A can be calculated by Eq. 4 as follows:

$$A = 24.56h_c^2 \tag{4}$$

where h_c is the true contact depth.

The nanoindentation tests were carried out as follows. A strain rate of 0.05 s^{-1} was maintained constant during the increment of load until the indenter reached a depth of 5000 nm into the surface. The load was then held at maximum value for 60 s in order to avoid the creep significantly affecting the unloading behaviour. The indenter was withdrawn from the surface at the same rate until 10% of the maximum load, followed by the indenter being completely removed from the material. Here, constant strain rate was chosen to load the samples in order to avoid strain-hardening effects on the measurements [9]. At least 40 indents were performed on each sample and the distance between the indentations was 50 μm to avoid interaction.

These materials were stressed at 5.0 kPa, which is the maximum value at which the hybrid material is approximately stressed in clinical use for the repair hard tissues [10]. The mechanical tests were carried out with an MTS-Adamel electromechanical testing machine. A load cell of 1 kN was used because it has greater sensitivity in the force values that must be applied to maintain these levels of stress. The strain values were determined at different times. To control the strain a laser extensometer was used. This type of extensometer was used with the aim that the pressure should not cause cuts in the material and therefore affect the values of the strain measured. With the laser extensometer fluorescent tapes were placed on the sample to be measured in order to allow the laser to measure the displacement values remotely.

With the aim of carrying out the mechanical tests in conditions similar to the human body, a physiological chamber was designed at a temperature of 37°C. The rate of application of the load to arrive at the stress studied was 1 mm/min and the rate of data acquisition by the Autotrack software was 25 points/s; this enabled us to control automatically the creep that is produced over time.

3 Results and discussion

3.1 Characterisation of ormosils

FTIR spectra of the different obtained ormosils showed the typical vibration bands of this type of organic–inorganic hybrid materials as it can be seen in Tables 3 and 4. In PDMS–$CaO–SiO_2$–PES ormosils (Table 3), the presence of the organic content within the network was confirmed by the presence of C–H stretching vibrations from CH_3 and CH_2 groups between 2960 and 2900 cm^{-1}. The presence of PDMS within the network was confirmed by the presence of the symmetric CH_3 deformation bands at ca. 1260 cm^{-1} together with the Si–CH_3 deformations at ca. 845 cm^{-1}. The inorganic network composed of Si–O–Si bonds was confirmed by the presence of typical asymmetric Si–O–Si stretching vibrations at ca. 1010 cm^{-1} and symmetric vibrations of Si–O bonds at ca. 795 cm^{-1}. The presence of phosphorous into the network was confirmed by the stretching P=O vibrations at ca. 1330 cm^{-1} and stretching vibrations from P–C bonds at ca. 600 cm^{-1}. It is important to highlight that no adsorption bands of nitrate ions coming at as by-products were present in the spectra (Fig. 5). This indicated that nitrates were eliminated during the washing and drying processes and never remained in the hybrid materials network. Thus, the possible toxicity because of the presence of nitrates can be here dismissed.

The $CaO–SiO_2$–PDMS ormosils FTIR spectra, Table 4, confirmed the incorporation of DDS units by the vibration bands of C–H stretching from CH_3 groups at ca. 2975-2930 cm^{-1}, Si–CH_3 deformation bands at ca. 1420 and

Table 3 Wavenumbers (cm^{-1}) and assignation of FTIR adsorption bands of PDMS–CaO–SiO_2–PES ormosils

$NP_{0.05-4}$	$NP_{0.10-2}$	$NP_{0.10-3}$	$NP_{0.10-4}$	Vibration mode	Assignation
3600–3000 (s, br)	3600–3000 (s, br)	3600–3000 (s, br)	3650–3000 (s, br)	OH, H	OH envelope
2963 (m)	2960 (m)	2961 (m)	2963 (m)	ν_{as}(C–H)	$-CH_2-R$
2907 (m)	2908 (m)	2907 (m)	2906 (m)	ν_s(C–H)	$-CH_2-R$
1631 (m, br)	1632 (m, br)	1634 (m, br)	1636 (m, br)	δ(H–O–H)	H_2O
1421 (m)	1425 (m)	1421 (m)	1445 (m)	δ_{as}(Si–CH_3)	≡Si–CH_3
1411 (m)	1412 (m)	1415 (m)	1416 (m)	ν(Si–C)	≡Si–CH_2
1333 (s)	1336 (s)	1332 (s)	1339 (s)	ν(P=O)	$(RO)_3P=O$
1259 (s, sh)	1258 (s, sh)	1258 (s, sh)	1258 (s, sh)	δ_s(Si–CH_3)	≡Si–CH_3
1012 (s, br)	1010 (s, br)	1012 (s, br)	1013 (s, br)	ν_{as}(Si–O–Si)	≡Si–O–Si≡
846 (s)	845 (s)	844 (s)	846 (s)	δ(Si–C)	–Si$(CH_3)_2$–O
793 (s)	794 (s)	792 (s)	793 (s)	ν(Si–O)	Si–O–Si
606 (w)	601 (w)	606 (w)	584 (w)	ν(P–C)	P–CH_2–
453 (w)	448 (w)	451 (w)	424 (w)	δ(Si–O–Si)	–O–Si–O–

Table 4 Wavenumbers (cm^{-1}) and assignation of FTIR adsorption bands of CaO–SiO_2–PDMS ormosils

$H_{N-0.25}$	H_{N-1}	$H_{N-1.5}$	Vibration mode	Assignation
3700–3100 (s, br)	3700–3100 (s, br)	3600–3000 (s, br)	OH, H	OH envelope
2974 (m)	2973 (m)	2971 (m)	ν_{as}(C–H)	CH_3-R
2928 (m)	2932 (m)	2935 (m)	ν_s(C–H)	CH_3-R
1636 (m, br)	1625 (m, br)	1628 (m, br)	δ(H–O–H)	H_2O
1426 (m)	1419 (m)	1421 (m)	δ_{as}(Si–CH_3)	≡Si–CH_3
1272 (s, sh)	1273 (s, sh)	1268 (s, sh)	δ_s(Si–CH_3)	≡Si–CH_3
1078 (s, br)	1089 (s, br)	1069 (s, br)	ν_{as}(Si–O–Si)	≡Si–O–Si≡
857 (s)	853 (s)	861 (s)	δ(Si–C)	–Si$(CH_3)_2$–O
812 (s)	812 (s)	809 (s)	ν(Si–O)	Si–O–Si
456 (w)	441 (w)	453 (w)	δ(Si–O–Si)	–O–Si–O–

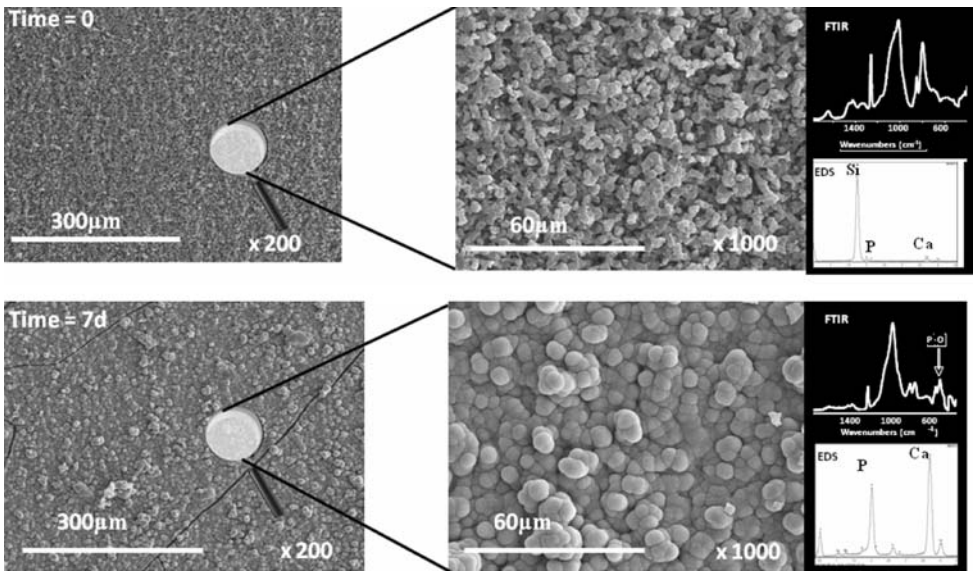

Fig. 5 SEM micrographs and the corresponding FTIR and EDS spectra of $NP_{0.10-2}$ surface before (*top*) and after (*bottom*) soaking into simulated body fluid for 7 days

1270 cm^{-1} and Si–C deformation bands at ca. 860 cm^{-1}. The formation of the silica network within the organic–inorganic hybrid was confirmed by the presence of the typical asymmetric Si–O–Si stretching vibrations at ca. 1010 cm^{-1} and symmetric vibrations of Si–O bonds at ca. 810 cm^{-1}. In the FTIR spectra of the hybrids of this series,

it was also confirmed the absence of bands assignable to nitrates coming from the calcium source.

In both types of ormosils, EDS experiments confirmed the incorporation of calcium into the network, as it is shown in Fig. 5 for the case of $NP_{0.10-2}$.

3.2 Bioactive behaviour of ormosils

The bioactive behaviour of these organic–inorganic hybrid materials was investigated attending to the changes of morphology and composition of the surface of the monoliths after soaking them into a simulated body fluid at 37°C for several days. SEM micrographs of materials after being soaked in SBF for 7 days showed the formation of a new layer covering the surface of the monolith (Fig. 5). This new layer was built of spherical particles and composed of calcium phosphate, as FTIR and EDS revealed (Fig. 5). The Ca/P molar ratio in this newly formed layer was found to range between 1.4 and 1.7 for different samples, which is within the typical range of values of biological apatites [11].

3.3 Mechanical properties of ormosils

The introduction of DEPETES into this type of ormosils promoted a higher degree of cross-linking because the additive was acting as a network former [5]. This cross-linking effect produces a structure with more stiffness and, due to the low mobility of the chains, the material presents low strain values when the sample is loaded. This fact can be observed in Table 5, where the increment of the elastic modulus (E), maximum strength (P_{max}) and hardness (H) increase with the DEPETES content.

Also the water content during the sol–gel formation of the NP monoliths has been revealed as an important factor over some mechanical properties (Table 6). Thus, the increase of the water content produces an important increase of the elastic modulus and the maximum strength. This fact is due to the fact that increasing the water content promotes the hydrolysis rate which leads to the formation of P–O–Si bonds reticulating the structure.

However, for the case of $CaO–SiO_2$–PDMS ormosils, it has been observed that the increase of DDS content produces a decrease of the mechanical properties (Table 7).

Table 5 Elastic modulus (E), maximum strength (P_{max}) and hardness (H) of PDMS–CaO–SiO_2–PES ormosils with different DEPETES content

Ormosils	DEPETES	H_2O	E (MPa)	P_{max} (kPa)	H (MPa)
$NP_{0.05-4}$	0.05	4	3.16 ± 0.44	13.02 ± 5.58	0.51
$NP_{0.10-4}$	0.10	4	4.67 ± 0.62	208.6 ± 21.88	0.70

Table 6 Elastic modulus, maximum strength and hardness of PDMS–CaO–SiO_2–PES ormosils with different water content

Ormosils	DEPETES	H_2O	E (MPa)	P_{max} (kPa)	H (MPa)
$NP_{0.10-2}$	0.10	2	1.89 ± 0.58	80.02 ± 9.69	0.44
$NP_{0.10-3}$	0.10	3	4.5 ± 0.44	166 ± 8.46	0.62
$NP_{0.10-4}$	0.10	4	4.67 ± 0.62	208.6 ± 21.88	0.70

Table 7 Elastic modulus, maximum strength and hardness of $CaO–SiO_2$–PDMS ormosils with different DDS content

Ormosils	TEOS	DDS	E (MPa)	P_{max} (kPa)	H (MPa)
$H_{0.25}$	1	0.25	8.32 ± 0.95	181.89 ± 10.89	0.92
H_1	1	1	5.15 ± 0.61	30.67 ± 7.14	0.79
$H_{1.5}$	1	1.5	3.71 ± 0.21	172.22 ± 9.45	0.59

Such behaviour could be explained by the different reaction rate of DDS compared to TEOS, so large amounts of DDS would favour homo-condensation rather than poly-condensation. This would lead to a negative influence on the formation of a homogeneous material, and the mechanical properties of the resultant high concentrated DDS monoliths would be decreased.

Figures 6 and 7 show the creep at constant stress of 5.0 kPa. In view of the results, it can be seen that the same potential rule of the increase of the strain with time is produced. As was to be expected, to achieve a level of stationary strain behaviour is necessary at shorter time for the H samples than NP samples. For the samples $NP_{0.05-4}$ this stationary behaviour is not observed due to the low value of strength.

The strain saturation levels—i.e., the time at which the stress becomes practically constant with time—are more important when the Young's moduli are high. The maximum value for NP samples corresponds to $NP_{0.10-4}$ with

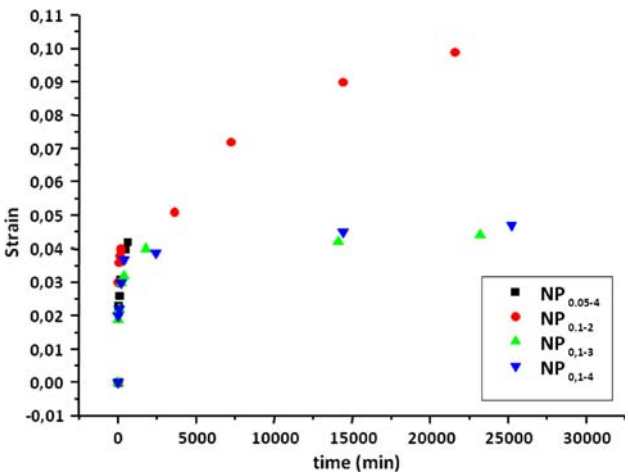

Fig. 6 Strain versus time plot of PDMS–CaO–SiO_2–PES ormosils

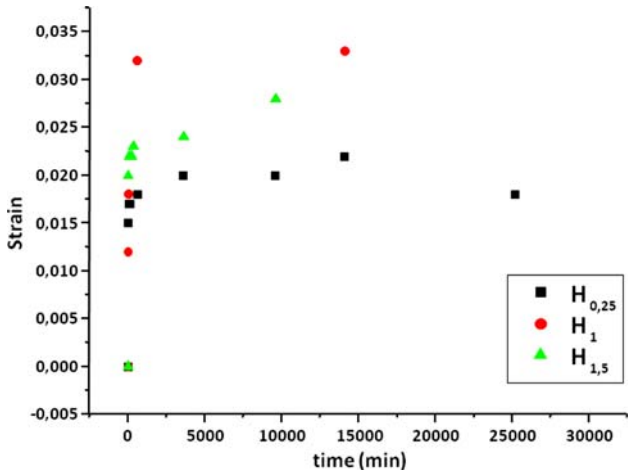

Fig. 7 Strain versus time plot of $CaO–SiO_2$–PDMS ormosils

4.67 MPa and for the H series corresponds to the $H_{0.25}$ with 8.3 MPa. Note the great speed with which the H materials increase their strain and reach constant strain values. This is a positive factor in that clinics will know that the strain a certain stress in a short time of approximately 500 s.

4 Conclusions

The mechanical properties of $CaO–SiO_2$–PDMS ormosils have been investigated in terms of nanoindentation. Different additives to these ormosils, such as DEPETES and DDS, and their effect over the mechanical properties of these materials have been also investigated. When the amount of DEPETES added was incremented, an increase in some mechanical properties such as elastic modulus, maximum strength and hardness was observed. This trend was similar when increasing the amount of water. The mechanical behaviour of these hybrids has been observed to be visco-elastic, and the subsequent creep phenomena have been seen to be accelerated at physiological temperature of 37°C.

Acknowledgments Financial support of CICYT (Spain) through research projects MAT2008-736 and MAT2007-61927, Comunidad de Madrid (Spain) through S-505-MAT-0324 research action is acknowledged.

References

1. Hench LL. Bioceramics: from concept to clinic. J Am Ceram Soc. 1991;74:1487–510. doi:10.1111/j.1151-2916.1991.tb07132.x.
2. Vallet-Regí M, Ragel CV, Salinas AJ. Glasses with medical applications. Eur J Inorg Chem. 2003;6:1029–42. doi:10.1002/ejic.200390134.
3. Kamitakahara M, Kawashita M, Miyata N, Kokubo T, Nakamura T. Bioactivity and mechanical properties of polydimethylsiloxane (PDMS)–CaO–SiO_2 hybrids with different PDMS contents. J Sol–Gel Sci Technol. 2001;21:75–81. doi:10.1023/A:1011261617377.
4. Hijón N, Manzano M, Salinas AJ, Vallet-Regí M. Bioactive CaO–SiO_2–PDMS coatings on Ti6Al4V substrates. Chem Mater. 2005;17(6):1591–6. doi:10.1021/cm048755i.
5. Manzano M, Salinas AJ, Vallet-Regí M. P-containing ORMOSILS for bone reconstruction. Prog Solid State Chem. 2006;34:267–77. doi:10.1016/j.progsolidstchem.2005.11.045.
6. Salinas AJ, Merino JM, Babonneau F, Gil FJ, Vallet-Regí M. Microstructure and macroscopic properties of bioactive CaO–SiO_2–PDMS hybrids. J Biomed Mater Res Part B Appl Biomater. 2007;81:274–82. doi:10.1002/jbm.b.30663.
7. Kokubo T, Kushitani H, Sakka S, Kitsugi T, Yamamuro TJ. Solutions able to reproduce in vivo surface-structure changes in bioactive glass-ceramic A-W^3. J Biomed Mater Res. 1990;24:721–34. doi:10.1002/jbm.820240607.
8. Sneddon IN. The relation between load and penetration in the axisymmetric boussinesq problem for a punch of arbitrary profile. Int J Eng Sci. 1965;3:47–57. doi:10.1016/0020-7225(65)90019-4#.
9. Beake BD, Chen S, Hull JB, Gao F. Nanoindentation behavior of clay/poly(ethylene oxide) nanocomposites. J Nanosci Nanotechnol. 2002;2:73–9. doi:10.1166/jnn.2002.077.
10. Meaney DF. Mechanical properties of implantable biomaterials. Clin Podiatr Med Surg. 1995;12:363–84. PMID: 7553529.
11. Ravaglioli A, Krajewski A, Celotti GC, Piancastelli A, Bacchini B, Montanari L, et al. Mineral evolution of bone. Biomaterials. 1996;17:617–22. doi:10.1016/0142-9612(96)88712-6.